BNL-101976-2014-TECH
AD/RHIC/64;BNL-101976-2013-IR

Closed Orbit Analysis for RHIC Insertion

S. Y. Lee

January 1990

Collider Accelerator Department
Brookhaven National Laboratory

U.S. Department of Energy
USDOE Office of Science (SC)

DISCLAIMER

AD/RHIC–64

R H I C P R O J E C T

Brookhaven National Laboratory
Associated Universities, Inc.
Upton, NY 11973

Closed Orbit Analysis for RHIC Insertion

S.Y. Lee and S. Tepikian

February 1990

Closed Orbit Analysis for RHIC Insertion

S.Y. Lee and S. Tepikian
Accelerator Development Department

ABSTRACT

Analytic closed orbit analysis is performed to evaluate the tolerance of quadrupole misalignment and dipole errors (b_0 and a_0) in the RHIC insertion. Sensitivity coefficients of these errors are tabulated for different β^* values. Using these sensitivity tables, we found that the power supply ripple of 10^{-4} can cause closed orbit motion of 0.05 mm at the IP in comparison with the rms beam size of 0.3 mm. It is desirable to have the power supply ripple less than 10^{-5}.

1. Introduction

The closed orbit error in the insertion region is fundamental importance to the collider physics. For RHIC, the closed orbit at the high–β triplets may also affect the dynamical aperture. Evaluation of the sensitivity on the quadrupole alignment errors and dipole excitation or rotation angle error can give us a feeling of the alignment tolerance. Some correction schemes may also be applied to obtain proper orbit control in the insertion region.

Figure 1 shows the RHIC insertion layout. There are nine quadrupoles on both sides of the interaction point (IP). The closed orbit can result from (1) quadrupole misalignment, (2) dipole error, etc. In the following section, we discuss the method of analysis.

2. Method of Orbit Error Analysis

For a particle in the accelerator, the equation of motion is given by

$$\frac{d^2x}{ds^2} + K(s)x = \frac{\Delta B(s)}{B\rho} \tag{1}$$

where

$$K(s) = \frac{\partial B_x/\partial x}{B\rho} \tag{2}$$

and $\Delta B(s)$ is the error field. For the horizontal closed orbit, $\Delta B(s)$ arises from: (h1) particles with closed orbits shifted horizontally from the center of a quadrupole or quadrupole

horizontal misalignments and (h2) dipole excitation error. For the vertical closed orbit, $\Delta B(s)$ arises from: (v1) particles with closed orbits shifted vertically from the center of a quadrupole or a quadrupole vertical misalignment and (v2) dipole rotation. We assume first that the beam exits from the arc at Q9 with phase space coordinates (x_9,x_9') [similarly (y_9,y_9') for vertical motion]. The closed orbit or the beam can be obtained by integrating Eq. (1) along the beam line with the proper quadrupole and dipole strengths and preassumed errors. We denote the misalignment errors of the quadrupoles, Q1 to Q8 as $\Delta_1, \Delta_2, \ldots, \Delta_8$ respectively. The percentage dipole excitation errors are $\Delta\theta/\theta$, $\Delta\theta_s/\theta_s$, $\Delta\theta_{c2}/\theta_{c2}$ and $\Delta\theta_{c1}/\theta_{c1}$ for the dipoles B, BSI(O), BC2 and BC1 respectively shown in Fig. 1. The method of integrating Eq. (1) is a standard initial value problem. Furthermore, we use the thin lens approximation in integrating Eq. (1). We shall find the phase space coordinates at locations, Q5, Q3, Q2, Q1 and IP as a function of initial condition (x_9,x_9') and the dipole error parameters.

3. Horizontal Closed Orbit Error

Table 1 lists the sensitivity coefficients for the horizontal closed orbit error at Q5, Q3, Q2, Q1 and IP as a function of the error fields discussed in section 2. As an example, the table corresponding to $\beta^* = 2$ m gives

$$x_3 = -7\ x_9 - 123\ x_9' + 2.72\ \Delta_8 - 12.5\ \Delta_7 + \\ + 3.5\ \frac{\Delta\theta}{\theta} + 4.26\ \Delta_6 + 1.1\ \frac{\Delta\theta_s}{\theta_s} - 8.17\ \Delta_5 + 5.76\ \Delta_4$$

and

$$x_{IP} = 1.3\ x_9 + 18.1\ x_9' - 0.97\ \Delta_8 + 3.32\ \Delta_7 - 0.85\ \frac{\Delta\theta}{\theta} \\ - 0.85\ \Delta_6 - 0.18\ \frac{\Delta\theta_s}{\theta_s} + 1.14\ \Delta_5 - 0.53\ \Delta_4 - 2.62\ \Delta_3 \\ + 3.18\ \Delta_2 - 2.37\ \Delta_1 + 0.30\ \frac{\Delta\theta_{c2}}{\theta_{c2}} + 0.21\ \frac{\Delta\theta_{c1}}{\theta_{c1}}$$

Fig. 2 gives a bar chart of the sensitivity of each error field.

We observe clearly that the closed orbit at Q3 (similarly at Q2 and Q1) is very sensitive to x_9'. A 0.1 mrad error in x_9' can give rise to 12 mm error at Q3 location by assuming a perfect machine. Besides x_9', x_3 is also sensitive to quadrupole misalignments. A 0.25 mm alignment in Q7, Q6, Q5 and Q4 can cause 4 mm rms closed orbit error at Q3. Similarly proper Q1–Q3 quadrupole alignment is important to the closed orbit at IP.

Figures 3 and 4 shows the similar sensitivity bar chart for $\beta^* = 6$ m and 0.5 m respectively. Note the vertical scale change in the $\beta^* = 0.5$ m case.

The table also gives us a guide line for the stability requirement in the power supply. As an example at $\beta^* = 2$ m, we find

$$x_{IP} = -0.85\,\frac{\Delta\theta}{\theta} - 0.18\,\frac{\Delta\theta_s}{\theta_s} + 0.30\,\frac{\Delta\theta_{c2}}{\theta_{c2}} + 0.21\,\frac{\Delta\theta_{c1}}{\theta_{c1}}$$

from table 1. A power supply ripple will affect $\Delta\theta/\theta$ for all dipole coherently. At $\Delta\theta/\theta \simeq 10^{-4}$, we expect the orbit will be shifted by 0.05 mm in comparison with the $\sigma_{\text{beam size}} \simeq 0.3$ mm. The effect will be very harmful to the beam life time due to the presence of beam–beam interaction. It is therefore important to achieve the power supply ripple less than $\frac{\Delta\theta}{\theta} \leq 10^{-5}$. At $\beta^* = 0.5$ m, table 1 gives

$$x_{IP}(\beta^* = 0.5\text{ m}) = -1.8\,\frac{\Delta\theta}{\theta} = 0.31\,\frac{\Delta\theta_x}{\theta_s} + 0.30\,\frac{\Delta\theta_{c2}}{\theta_{c2}} + 0.21\,\frac{\Delta\theta_{c1}}{\theta_{c1}} \quad .$$

At $\Delta\theta/\theta \simeq 10^{-5}$ ripple will give $\Delta x_{IP} \simeq 0.02$ mm in comparison with the proton beam size $\sigma = 0.08$ mm. Thus the power supply stability is especially important to the proton collision mode.

4. Vertical Closed Orbit

Table 2 lists the similar sensitivity table for the vertical closed orbit motion by integrating Eq. (1) along the insertion, where the quadrupole vertical misalignment is given by $\Delta_1, \ldots, \Delta_8$ and the dipole rotation is given by φ, φ_s, φ_{c2} and φ_{c1} for the corresponding dipoles B, BSI(0), BC2 and BC1 respectively.

Similar to that of the horizontal motion, the quadrupole alignment of Q1–Q3 is important to the proper collision at IP. Power supply ripple is also critical for the operation at $\beta^* \leq 2$ m.

5. Conclusion and Discussion

The closed orbit analysis for the RHIC insertion is analyzed in the analytic model in terms of the quadrupole alignment errors and the dipole errors. We calculate the sensitivity coefficients for various β^* values. The closed orbit error becomes large at the high–β quadrupoles, Q1–Q3. To minimize these error, one should properly align the quadrupoles in the insertion. One should also measure x_9, x'_9, y_9 and y'_9 so that a proper orbit correction scheme for the insertion can be established due to the fact that the closed orbit is sensitively dependent on the parameters x'_9 and y'_9 (see Tables 1 and 2).

Using the table, we can also set the tolerance on the power supply ripple. At low β^* value, the power supply ripple of 10^{-5} is critical to obtain a proper beam–beam collision.

Finally the ground motion due to the high tide, local traffic, etc. will shift quadrupole alignment. A shift of 10 μ in Q1–Q3 can also cause beam movement at the IP by 0.01 mm, which will affect the performance. Fortunately, the ground motions which does not change the relative motion of the accelerator component do not affect the luminosity. The random noise is however normally small, $\simeq 1$ μ. Thus the effect should not be important. Realistic measurement of the effect in RHIC tunnel should be confirmed.

Table 1 Sensitivity Coefficients of the Closed Orbit Displacement

β^*=0.5m	x_5	x'_5	x_3	x'_3	x_2	x'_2	x_1	x'_1	x_{IP}	x'_{IP}
x_9	-1	-0.1	-15.5	-0.3	-8.6	0.9	-10.3	-0.5	3.1	0.5
x'_9	-11.2	-2.2	-246	-4.8	-137	14.7	-164.	-7.6	46.4	8.6
Δ_8	1.06	0.02	8.57	0.16	4.71	-0.52	5.62	0.25	-1.89	-0.3
Δ_7	-3.37	-0.16	-34.2	-0.65	-18.8	2.06	-22.5	-1	7.19	1.2
$\Delta\theta/\theta$	0.79	0.05	8.68	0.17	4.8	-0.52	5.74	0.26	-1.8	-0.31
Δ_6	0.27	0.03	3.85	0.07	2.14	-0.23	2.56	0.12	-0.77	-0.13
$\Delta\theta_s/\theta_s$	0.07	0.01	1.63	0.03	0.91	-0.1	1.1	0.05	-0.31	-0.06
Δ_5			0	0	0	0	0	0	0	0
Δ_4			5.3	0.11	3.03	-0.3	3.72	0.19	-0.65	-0.18
Δ_3					-0.59	-0.08	-1.23	-0.17	-2.57	-0.05
Δ_2							0.6	0.16	3.16	0.1
Δ_1									-2.42	-0.1
$\Delta\theta_{c2}/\theta_{c2}$									0.30	0.02
$\Delta\theta_{c1}/\theta_{c1}$									0.21	0.01

β^* =2m	x_5	x'_5	x_3	x'_3	x_2	x'_2	x_1	x'_1	x_{IP}	x'_{IP}
x_9	-0.8	-0.1	-7	-0.1	-3.8	0.4	-4.6	-0.2	1.3	0.2
x'_9	-2.5	-1.5	-123.	-2.5	-69.1	7.3	-83.5	-3.9	18.1	4.1
Δ_8	1.46	0.06	2.72	0.04	1.4	-0.18	1.58	0.05	-0.97	-0.1
Δ_7	-3.91	-0.22	-12.5	-0.21	-6.7	0.79	-7.8	-0.3	3.32	0.45
$\Delta\theta/\theta$	0.9	0.06	3.5	0.06	1.88	-0.22	2.21	0.09	-0.85	-0.12
Δ_6	0.64	0.06	4.26	0.08	2.34	-0.26	2.78	0.12	-0.85	-0.15
$\Delta\theta_x/\theta_s$	0.07	0.01	1.1	0.02	0.61	-0.07	0.73	0.03	-0.18	-0.04
Δ_5			-8.17	-0.17	-4.59	0.48	-5.56	-0.26	1.14	0.27
Δ_4			5.76	0.12	3.3	-0.33	4.05	0.2	-0.53	-0.19
Δ_3					-0.59	-0.08	-1.23	-0.17	-2.62	-0.06
Δ_2							0.6	0.16	3.18	0.1
Δ_1									-2.37	-0.1
$\Delta\theta_{c2}/\theta_{c2}$									0.30	0.02
$\Delta\theta_{c1}/\theta_{c1}$									0.21	0.01

Table 1 – continued

β^*=3m	x_5	x'_5	x_3	x'_3	x_2	x'_2	x_1	x'_1	x_{IP}	x'_{IP}
x_9	-1	-0.1	-5.2	-0.1	-2.9	0.3	-3.4	-0.1	1	0.2
x'_9	-7	-1.7	-112.	-2.2	-63.6	6.6	-77	-3.6	16	3.8
Δ_8	1.52	0.07	0.07	-0.02	-0.1	-0.02	-0.24	-0.04	-0.63	-0.02
Δ_7	-4.4	-0.26	-5.36	-0.05	-2.65	0.36	-2.88	-0.06	2.43	0.22
$\Delta\theta/\theta$	0.96	0.06	1.72	0.02	0.89	-0.11	1.01	0.03	-0.6	-0.07
Δ_6	0.85	0.08	3.62	0.06	1.99	-0.22	2.36	0.1	-0.77	-0.13
$\Delta\theta_s/\theta_s$	0.07	0.01	0.91	0.02	0.51	-0.05	0.62	0.03	-0.14	-0.03
Δ_5			-9.93	-0.2	-5.68	0.57	-6.93	-0.34	1.16	0.33
Δ_4			5.38	0.12	3.13	-0.3	3.87	0.2	-0.37	-0.17
Δ_3					-0.58	-0.08	-1.21	-0.17	-2.56	-0.05
Δ_2							0.59	0.16	3.15	0.1
Δ_1									-2.38	-0.1
$\Delta\theta_{c2}/\theta_{c2}$									0.30	0.02
$\Delta\theta_{c1}/\theta_{c1}$									0.21	0.01

β^*=6m	x_5	x'_5	x_3	x'_3	x_2	x'_2	x_1	x'_1	x_{IP}	x'_{IP}
x_9	-1.2	-0.1	-1.9	0	-1	0.1	-1.1	0	0.7	0.1
x'_9	-11.8	-2	-81.2	-1.5	-46.8	4.6	-57.5	-2.9	14.5	2.9
Δ_8	1.44	0.06	-4.03	-0.1	-2.52	0.2	-3.26	-0.2	-0.09	0.13
Δ_7	-4.5	-0.27	7.25	0.21	4.72	-0.34	6.26	0.42	0.94	-0.22
$\Delta\theta/\theta$	0.96	0.06	-1.02	-0.03	-0.69	0.04	-0.94	-0.07	-0.26	0.03
Δ_6	0.85	0.08	1.13	0.01	0.58	-0.07	0.66	0.02	-0.48	-0.05
$\Delta\theta_s/\theta_s$	0.07	0.01	0.67	0.01	0.39	-0.04	0.48	0.02	-0.11	-0.02
Δ_5			-12.0	-0.24	7.09	0.66	-8.86	-0.48	1.45	0.42
Δ_4			4.82	0.1	2.9	-0.26	3.66	0.21	-0.36	-0.16
Δ_3					-0.56	-0.08	-1.17	-0.17	-2.33	-0.05
Δ_2							0.59	0.16	3.09	0.1
Δ_1									-2.5	-0.1
$\Delta\theta_{c2}/\theta_{c2}$									0.30	0.02
$\Delta\theta_{c1}/\theta_{c1}$									0.21	0.01

Table 2 Sensitivity Coefficients of the Vertical Closed Orbit

β^*=0.5m	y_5	y'_5	y_3	y'_3	y_2	y'_2	y_1	y'_1	y_{IP}	y'_{IP}
y_9	-1.4	-0.1	3.6	0.1	6.7	0.4	4.2	-0.7	-2.5	-0.3
y'_9	18	-0.1	-79.3	-2.1	-141.	-8.4	-87.9	14.6	60.5	6
Δ_8	-4.5	-0.1	17.08	0.48	30.71	1.83	19.11	-3.15	-12.5	-1.28
Δ_7	2.44	0.07	-8.78	-0.25	-15.8	0.95	-9.86	1.62	6.36	0.66
φ	0.62	0.03	-1.94	-0.06	-3.53	-0.21	-2.2	0.36	1.35	0.14
Δ_6	-0.27	-0.03	0.55	0.02	1.03	0.06	0.65	-0.1	-0.31	-0.04
φ_s	0.07	0.01	0.02	0	0.01	0	0	0	-0.08	0
Δ_5			0	0	0	0	0	0	0	0
Δ_4			-5.3	-0.11	-9.27	-0.53	-5.7	0.97	4.49	0.41
Δ_3					0.59	0.08	0.53	-0.02	1.4	0.04
Δ_2							-0.6	-0.16	-6.05	-0.22
Δ_1									2.42	0.1
φ_{c2}									0.30	0.02
φ_{c1}									0.21	0.01

β^*=2m	y_5	y'_5	y_3	y'_3	y_2	y'_2	y_1	y'_1	y_{IP}	y'_{IP}
y_9	-1.1	0	2.5	0.1	4.7	0.3	3	-0.5	-1.5	-0.2
y'_9	9.4	-0.8	-40.8	-1.1	-73.1	-4.3	-45.5	7.5	31.8	3.1
Δ_8	-3.21	0.03	9.31	0.31	17.05	1.04	10.72	-1.72	-6.34	-0.69
Δ_7	1.77	0.01	-4.52	-0.16	-8.36	-0.52	-5.27	0.84	2.91	0.33
φ	0.51	0.02	-0.95	-0.04	-1.8	-0.11	-1.15	0.18	0.5	0.07
Δ_6	-0.64	-0.06	0.42	0.04	0.94	0.07	0.64	-0.08	0.14	-0.02
φ_s	0.07	0.01	0.11	0	0.15	0.01	0.09	-0.02	-0.17	-0.01
Δ_5			2.07	0.03	3.54	0.2	2.16	-0.38	-2.02	-0.17
Δ_4			-5.76	-0.12	-10.0	-0.58	-6.2	1.05	5.04	0.45
Δ_3					0.59	0.08	0.53	-0.02	1.39	0.03
Δ_2							-0.6	-0.16	-6.01	-0.22
Δ_1									2.37	0.1
φ_{c2}									0.30	0.02
φ_{c1}									0.21	0.01

Table 2 – continued

β^*=3m	y_5	y'_5	y_3	y'_3	y_2	y'_2	y_1	y'_1	y_{IP}	y'_{IP}
x_9	-0.9	0	1.4	0.1	2.7	0.2	1.7	-0.3	-0.5	-0.1
y'_9	6.2	-1.1	-34.4	-0.8	-60.6	-3.5	-37.8	6.2	25.4	2.6
Δ_8	-2.55	0.1	6.34	0.22	11.62	0.71	7.38	-1.15	-3.57	-0.44
Δ_7	1.49	-0.02	-2.82	-0.11	-5.28	-0.33	-3.38	0.52	1.31	0.19
φ	0.44	0.01	-0.37	-0.03	-0.78	-0.05	-0.52	0.07	-0.02	0.02
Δ_6	-0.85	-0.08	-0.58	0.03	-0.72	-0.02	-0.36	0.1	1.18	0.06
φ_s	0.07	0.01	0.22	0	0.35	0.02	0.21	-0.04	-0.25	-0.02
Δ_5			2.84	0.05	4.83	0.27	2.96	-0.51	-2.5	-0.22
Δ_4			-5.38	-0.12	-9.36	-0.54	-5.81	0.97	4.25	0.41
Δ_3					0.58	0.08	0.52	-0.01	1.4	0.04
Δ_2							-0.59	-0.16	-5.95	-0.22
Δ_1									2.38	0.1
φ_{c2}									0.30	0.02
φ_{c1}									0.21	0.01

β^*=6m	y_5	y'_5	y_3	y'_3	y_2	y'_2	y_1	y'_1	y_{IP}	y'_{IP}
y_9	-0.9	0	-0.2	0	-0.1	0	0	0	0.8	0
y'_9	6.5	-1.1	-26.6	-0.7	-46.8	-2.7	-29.1	4.8	17.3	1.9
Δ_8	-2.59	0.1	2.15	0.14	4.38	0.3	2.89	-0.41	0.09	-0.11
Δ_7	1.52	-0.02	-0.27	-0.06	-0.89	-0.08	-0.67	0.06	-0.88	-0.01
φ	0.44	0.01	0.45	-0.01	0.63	0.02	0.34	-0.08	-0.69	-0.04
Δ_6	-0.85	-0.08	-2.32	-0.01	-3.67	-0.18	-2.17	0.41	2.53	0.19
φ_s	0.07	0.01	0.39	0	0.64	0.03	0.39	-0.07	-0.38	-0.03
Δ_5			4.03	0.07	6.8	0.37	4.14	-0.72	-3.34	-0.3
Δ_4			-4.82	-0.1	-8.29	-0.47	-5.1	0.87	3.59	0.35
Δ_3					0.56	0.08	0.51	-0.01	1.4	0.04
Δ_2							-0.59	-0.16	-6.05	-0.22
Δ_1									2.5	0.1
φ_{c2}									0.30	0.02
φ_{c1}									0.21	0.01

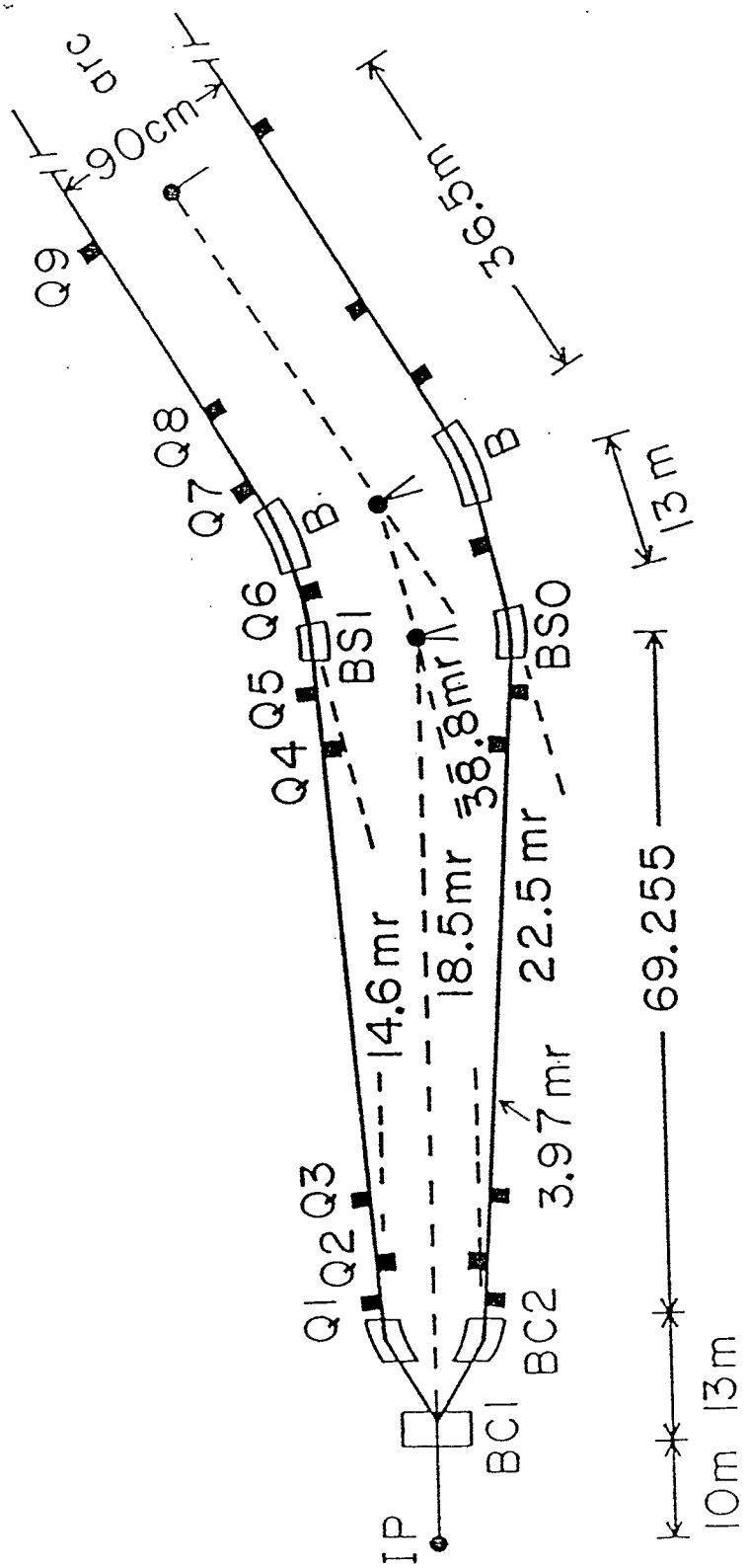

Expanded Layout of Half-Insertion.

Figure 1

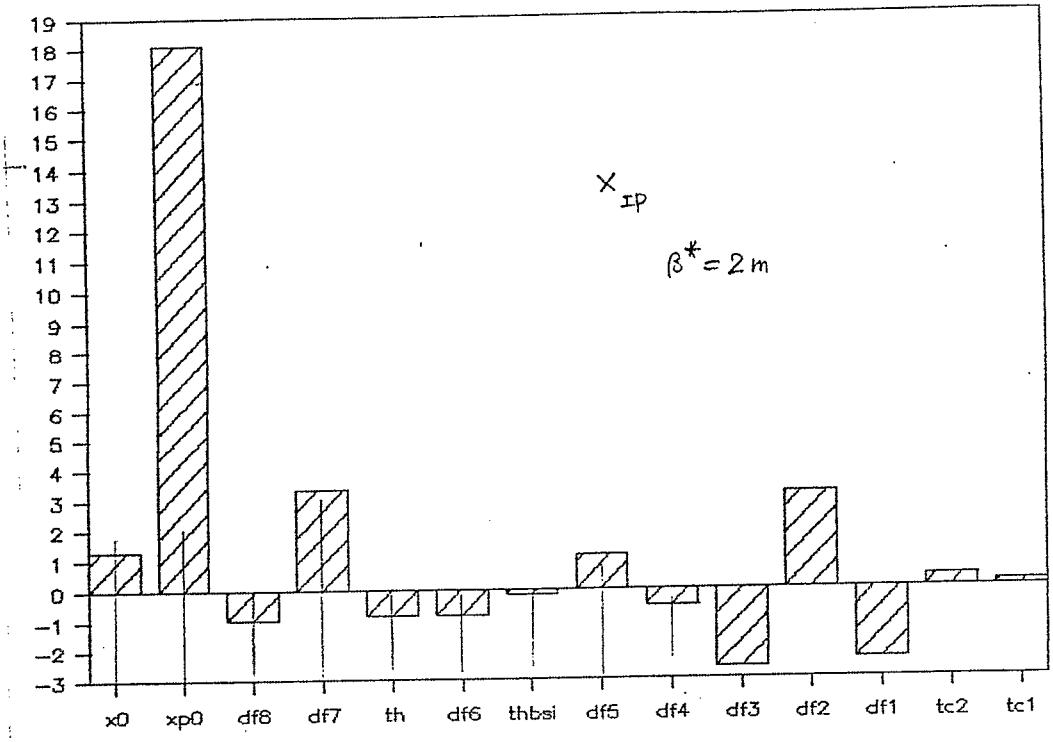
19
18
17
16
15
14
13
12
11
10
9
8
7
6
5
4
3
2
1
0
−1
−2
−3
X_{IP}
$\beta^* = 2\,m$
x0
xp0
df8
df7
th
df6
thbsi
df5
df4
df3
df2
df1
tc2
tc1

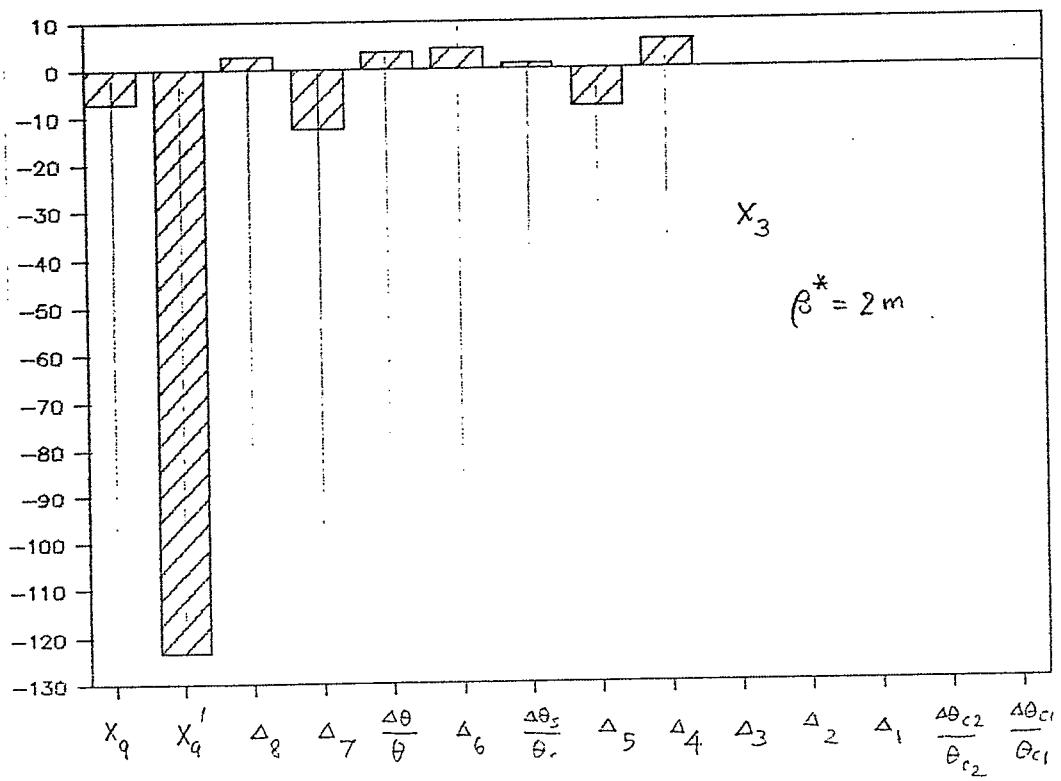
10
0
−10
−20
−30
−40
−50
−60
−70
−80
−90
−100
−110
−120
−130
X_3
$\beta^* = 2\,m$
X_q
X_q'
Δ_8
Δ_7
$\frac{\Delta\theta}{\theta}$
Δ_6
$\frac{\Delta\theta_5}{\theta_5}$
Δ_5
Δ_4
Δ_3
Δ_2
Δ_1
$\frac{\Delta\theta_{c2}}{\theta_{c2}}$
$\frac{\Delta\theta_{c1}}{\theta_{c1}}$

Figure 2

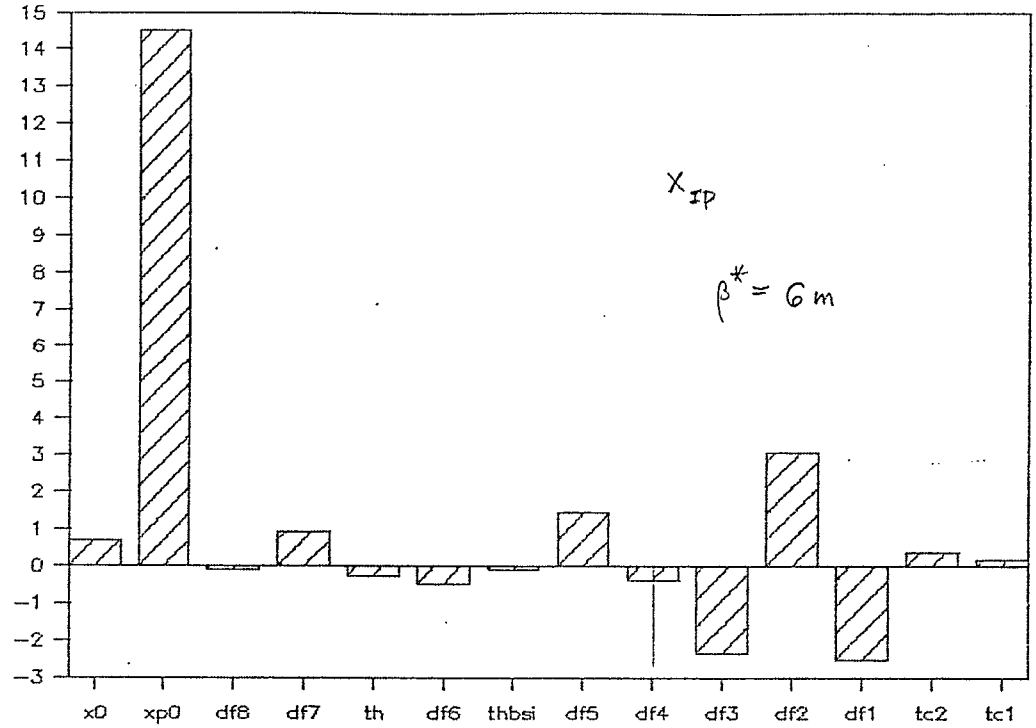
15
14
13
12
11
10
9
8
7
6
5
4
3
2
1
0
−1
−2
−3
X_{IP}
$\beta^* = 6\,m$
x0
xp0
df8
df7
th
df6
thbsi
df5
df4
df3
df2
df1
tc2
tc1

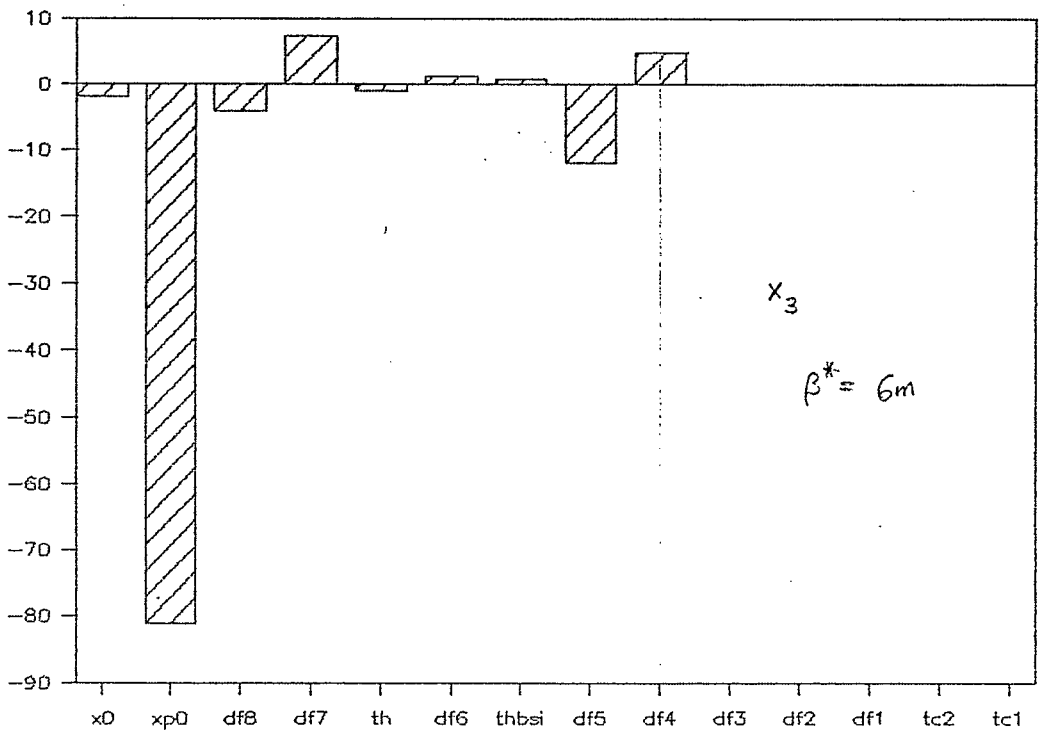
10
0
−10
−20
−30
−40
−50
−60
−70
−80
−90
X_3
$\beta^* = 6m$
x0
xp0
df8
df7
th
df6
thbsi
df5
df4
df3
df2
df1
tc2
tc1

Figure 3

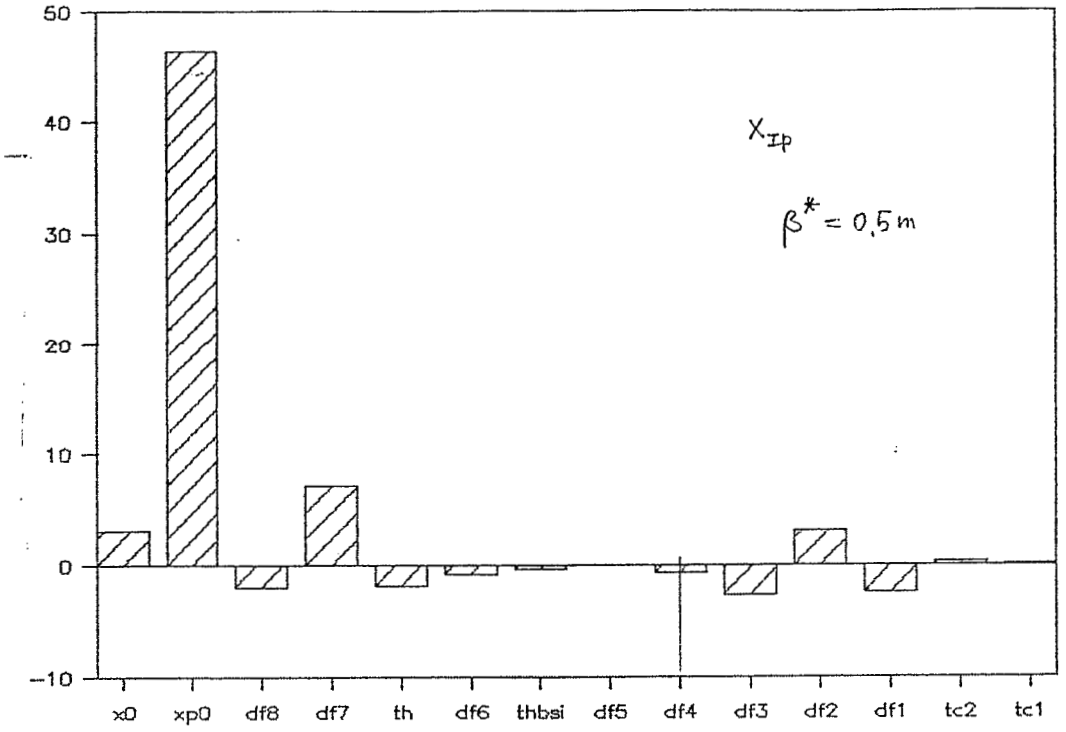
50
40
30
20
10
0
−10
X_{Ip}
$\beta^* = 0,5\,m$
x0
xp0
df8
df7
th
df6
thbsi
df5
df4
df3
df2
df1
tc2
tc1

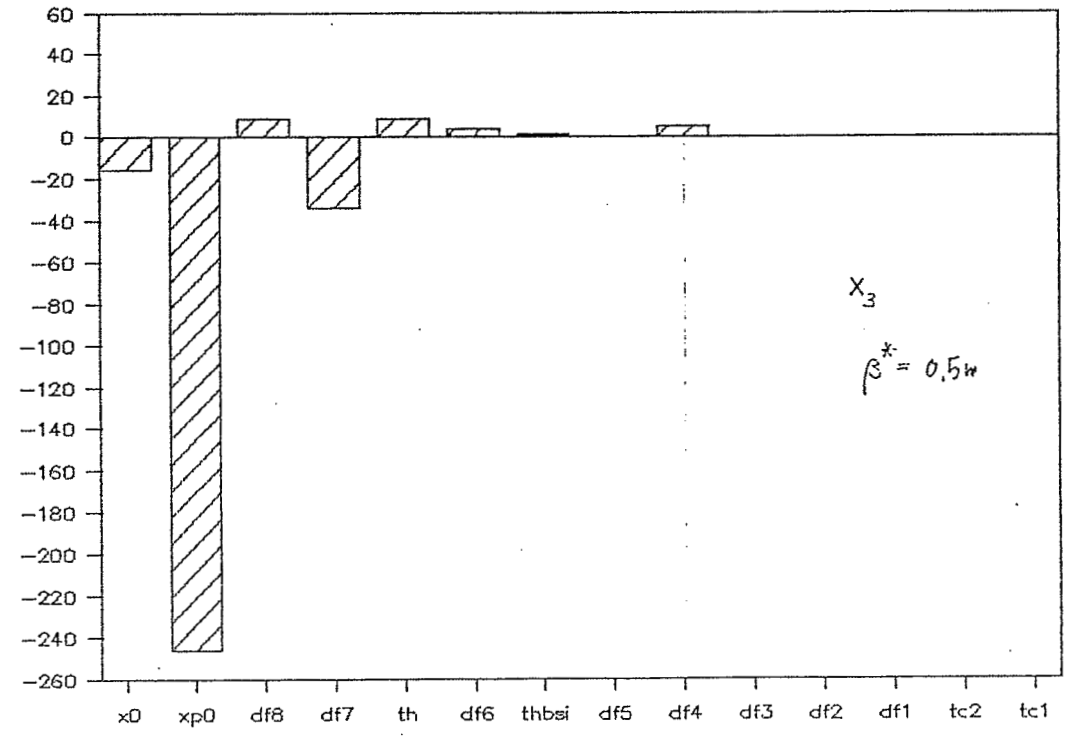
60
40
20
0
−20
−40
−60
−80
−100
−120
−140
−160
−180
−200
−220
−240
−260
X_3
$\beta^* = 0,5\,w$
x0
xp0
df8
df7
th
df6
thbsi
df5
df4
df3
df2
df1
tc2
tc1

Figure 4